JOURNAL OF MATERIALS SCIENCE 27 (1992) 2863–2872

Interface between zinc phosphate-deposited steel fibres and cement paste

T. SUGAMA, N. CARCIELLO, L. E. KUKACKA
Energy Efficiency and Conservation Division, Department of Applied Science, Brookhaven National Laboratory, Upton, NY 11973, USA

G. GRAY
Massachusetts Institute of Technology, Department of Mechanical Engineering, Cambridge, MA 02139, USA

In an attempt to protect steel fibre reinforcements from corrosion and improve their adherence to cement pastes, we deposited a zinc phosphate (ZnPh) conversion coating on the surface of the fibres. At the interfacial contact zones between the cement paste and ZnPh, alkali-induced dissolution caused the dissociation of abundant PO_4^{3-} ions from the ZnPh. The interaction of PO_4^{3-} ions with Ca^{2+} ions from the pastes led to the formation of hydroxyapatite and brushite in the vicinity of the dissolved ZnPh surface. Such intermediate calcium phosphate compounds played important roles in (1) improving the cement–fibre interfacial bonds, and (2) repairing the damage of the ZnPh surfaces dissolved by alkali. These processes protected the steel fibre from corrosion.

1. Introduction

Zinc phosphate (ZnPh) conversion coating is an inorganic crystalline coating that improves the adherent properties of carbon steel substrates and protects them against corrosion. We reported [1–3] that insoluble crystalline ZnPh coatings can be directly fabricated on a carbon steel surface by a dissolution–recrystallization process, using zinc orthophosphate dihydrate, $[Zn_3(PO_4)_2 \cdot 2H_2O]$ as a starting material. The precipitated ZnPh not only reduces the corrosion rate of the steel, but also provides an open surface topography that contributes to the strong mechanical interlocking bonds formed with the adhesive material.

Using conventional zinc-coating technology in terms of galvanization, several investigators [4–7] discussed corrosion protection and the adherence of zinc-coated (galvanized) steel embedded in cement paste. They found that when the Zn-coated steel came into contact with a highly alkaline interstitial fluid within the paste, the coatings were dissolved by the attack of alkaline hydroxide ions, OH^-. This dissolution of the Zn coatings led to the formation of porous ZnO or to the precipitation of $Zn(OH)_2$, which then was transformed into $Ca[Zn(OH)_2]_2 \cdot 2H_2O$, thereby resulting in the corrosion of galvanized steel. From the viewpoint of adherence to the cement, such dissolution–precipitation occurring at the coating–cement interfaces disrupted the interfacial bonds between the fibre and cement; this weakening was due mainly to the formation of a porous microstructure in the hydraulic cement adjacent to the Zn coating.

It is not surprising that ZnPh conversion coatings are also susceptible to alkali dissolution. In fact, the dissolution behaviour of ZnPh in alkali metal hydroxides was investigated by Sommer and Leidhesior [8] and ourselves [3]. We were agreed that the major ionic species that dissociates from the ZnPh coating at a pH of 13.0 is phosphate, PO_4^{3-}, with zinc, Zn^{2+}, ion as a minor species. Thus, our particular interest lies in the dissolution of PO_4^{3-} ions, which are known to be one of the corrosion inhibitors of steel reinforcements in concrete [9], at a similar pH within Portland cement paste [10]. Likewise, such reactive PO_4^{3-} anions may react with calcium cations liberated from the cement grains in an aqueous medium, and subsequently form an insoluble calcium phosphate compound such as brushite, $CaHPO_4 \cdot 2H_2O$ or hydroxyapatite, $Ca_5(PO_4)_3(OH)$ [11, 12]. We were interested to know whether the precipitation of these calcium phosphate compounds as an interfacial reaction product are active in the repair of damage at the dissolved ZnPh surface.

We selected steel fibre reinforcements that would give a practical demonstration of the application of ZnPh conversion techniques. Assuming that the ZnPh layer deposited on the fibre surfaces would be dissolved at the contact zone with the paste, our objective was to explain and explore the chemical and mechanical behaviour of the ZnPh conversion layer as an anticorrosive coating for steel fibre embedded in hydraulic cement. We investigated the ability of ZnPh coating to protect steel fibres from corrosion, and examined the microstructure and mechanisms involved in bonding at the interfacial regions between ZnPh and cement. The analytical tools used to obtain this information were scanning electron microscopy (SEM) coupled with energy dispersive X-ray spectrometry (EDX), and X-ray photoelectron spectroscopy (XPS).

0022–2461

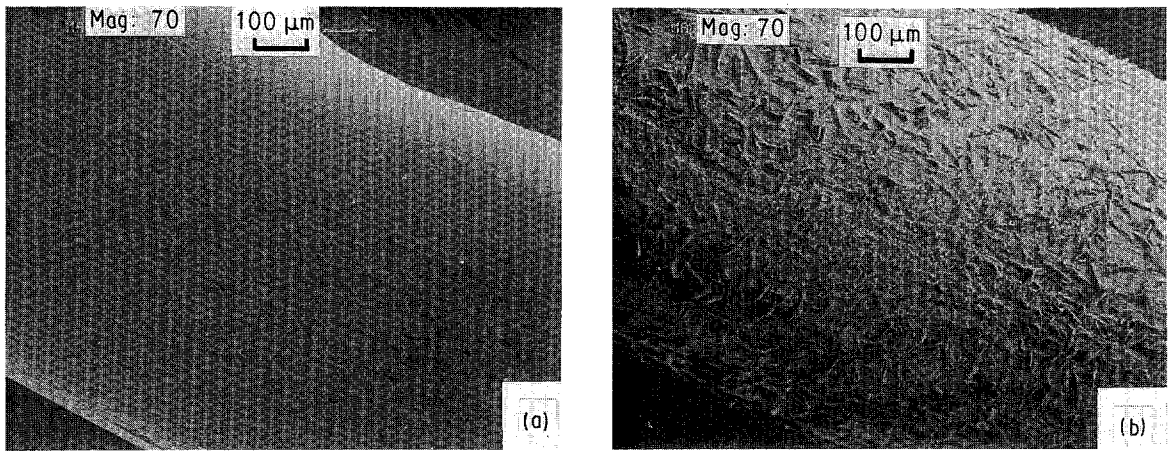

Figure 1 Scanning electron micrographs of (a) as-received steel fibre, and (b) ZnPh-treated fibre.

2. Experimental procedure

2.1. Materials

Wave-shaped steel fibres with a circular cross-section of 1.0 mm diameter, were used in this study. Before treating them with zinc phosphate and embedding in cement paste, the fibre surfaces were wiped with acetone-soaked tissues to remove any surface contaminants. The cement pastes were made from an ASTM Type I Portland cement with a water-to-cement ratio of 0.5.

The formulation for the zinc phosphating liquid used was 0.46 wt % zinc orthophosphate dihydrate, 0.91 wt % 85% H_3PO_4, and 98.63 wt % water. The ZnPh conversion coatings were prepared in the following way. First, the surface-cleaned fibre was immersed for 5 min in the ZnPh convertible solution described above, at a temperature of 90 °C. After immersion, the fibre surface was rinsed with water, and then dried in an oven at 150 °C for 10 min to remove any moisture.

Next, single fibre pull-out specimens were prepared by embedding a 12.5 mm long fibre in cement pastes having a size of 25 mm wide by 37.5 mm long by 12.5 mm thick. The fibre-embedded cement paste specimens then were placed in water at 25 °C for 3, 14, and 28 days. The resulting data on these specimens represent the average of three measurements.

2.2. Measurements

To gain information on the locus of interfacial bond failure, the microstructure, and the chemical composition at the critical interfacial zone between the hydrated cement paste and the fibre, we explored both the surface of fibres that had been removed from the paste and the surface of the grooves left by the fibres after they had been pulled out. We used an AMR10 nm scanning electron microscope (SEM) associated with TN-2000 energy-dispersion X-ray spectrometry (EDX), and X-ray photoelectron spectroscopy (XPS).

Quantitative analyses were made of the corrosion products formed on the ZnPh-treated and untreated surfaces of steel fibres after exposure to a 3% NaCl solution at 25 °C by measuring the binding energies and peak areas excited from XPS.

An Instron TIMB testing machine, which advanced at a crosshead speed of 0.13 cm min^{-1}, was used for all the fibre pull-out tests.

3. Results and discussion

3.1. Microstructure of steel fibre surfaces treated with zinc phosphate and protection against corrosion

Fig. 1 shows scanning electron micrographs for the as-received steel fibre (a) and zinc phosphate (ZnPh)-deposited fibre (b). It is apparent that the original smooth surface of the steel fibre was changed into a rough topographical feature by precipitating ZnPh crystals on the fibre. The high-resolution SEM and EDX spectra for the ZnPh-treated and untreated fibres are shown in Fig. 2. The typical surface morphology of an untreated fibre (Fig. 2a) exhibits numerous gutters ($\sim$ 5 μm wide) oriented along the fibre's axis. The accompanying EDX spectrum has an intense Fe signal and a weak peak of Ca; Ca is probably present as a contaminant. The gold element detected in the EDX spectrum is directly related to a gold film deposited on the SEM sample. The image of surface morphology for the ZnPh-treated fibre (Fig. 2b) expresses two distinguishable crystal features: one is that of plate-like crystals (b, 3), and the other is an agglomeration of granular-shaped crystals (b, 2). From the EDX elemental analyses, the former could be associated with the zinc phosphate compound $[Zn_3(PO_4)_2 \cdot 2H_2O]$ [3]. We interpret the latter as being iron-rich zinc phosphate compounds.

One of the major contributions of crystalline ZnPh coatings is to serve as a barrier to protect the steel fibre from corrosive reactants. We evaluated this ability by immersing the ZnPh-deposited steel fibre in an aerated 3% NaCl solution at 25 °C. For comparison, the "as-received" fibres were also immersed in the same solution. Quantitative data on ferric rust were obtained using XPS which is very suitable for analysing surface chemicals. In this study, the internally generated C_{1s}, O_{1s}, $Ca_{2p3/2}$, Fe_{2p} (area of entire doublet region), P_{2p}, and $Zn_{2p3/2}$ peak areas were used in obtaining the atomic fractions.

Table I shows the changes in chemical composition of the surface of as-received steel fibres after different lengths of exposure. The principal element of the unexposed surface was C, which probably belongs to the

TABLE I Changes in the chemical composition of the surface of steel fibres after exposure to 3% NaCl at 25 °C

Exposure time (h)	At %			
	C	O	Ca	Fe
0	53.3	38.6	5.4	2.7
1	56.0	39.0	1.4	3.6
2	54.1	40.5	0.8	4.6
5	50.4	41.5	0.0	8.1

C species in the fibres made from the carbon steel, and to C contaminants adsorbed from the atmosphere. The secondary dominant element was O, while the concentration of Ca contaminants was 5.4%, about twice as high as that of Fe. When the as-received fibres were exposed in the corrosive solutions, both the Fe and O elements became increasingly incorporated on to the surface of the fibre, whereas the concentration of Ca contaminants vanished within 5 h. The C atomic fraction varied in the range 50.4%–56.0%. This finding implies that the degree of coverage of the iron oxide compounds over the Ca-contaminated fibre surfaces progressively increases with extending exposure. Because the only source of Fe is the steel fibre, the oxidized iron compounds precipitated on the fibre can be interpreted as the familiar red–brown ferric rust, such as $Fe_2O_3 \cdot H_2O$ and FeO(OH) [13]. In fact, the change of the fibre surfaces to a red–brown colour could be observed visually in 5 h exposed samples. An inspection of the features of the high-resolution Fe_{2p} doublet separation spectrum (Fig. 3) for the unexposed and 5 h exposed samples strongly supported the findings described above. For all the XPS core level spectra, the scale of the binding energy (BE) was calibrated with the C_{1s} of the principal hydrocarbon-type carbon peak fixed at 285.0 eV as an internal reference standard. A curve deconvolution technique was employed to substantiate the information on the respective chemical state from the high-resolution spectra of each element, and to determine the relative quantity of a particular chemical state. In Fig. 3, the $Fe_{2p3/2}$ and $Fe_{2p1/2}$ lines at 710.7 and 724.3 eV excited from the unexposed fibre surfaces were attributable to the Fe element in the hydrated ferric oxide, $Fe_2O_3 \cdot H_2O$ [14]. This result directly reflected the fact that the as-received fibre surfaces have already been occupied by small amounts of ferric rust compounds. The considerable growth in peak intensity and area at the

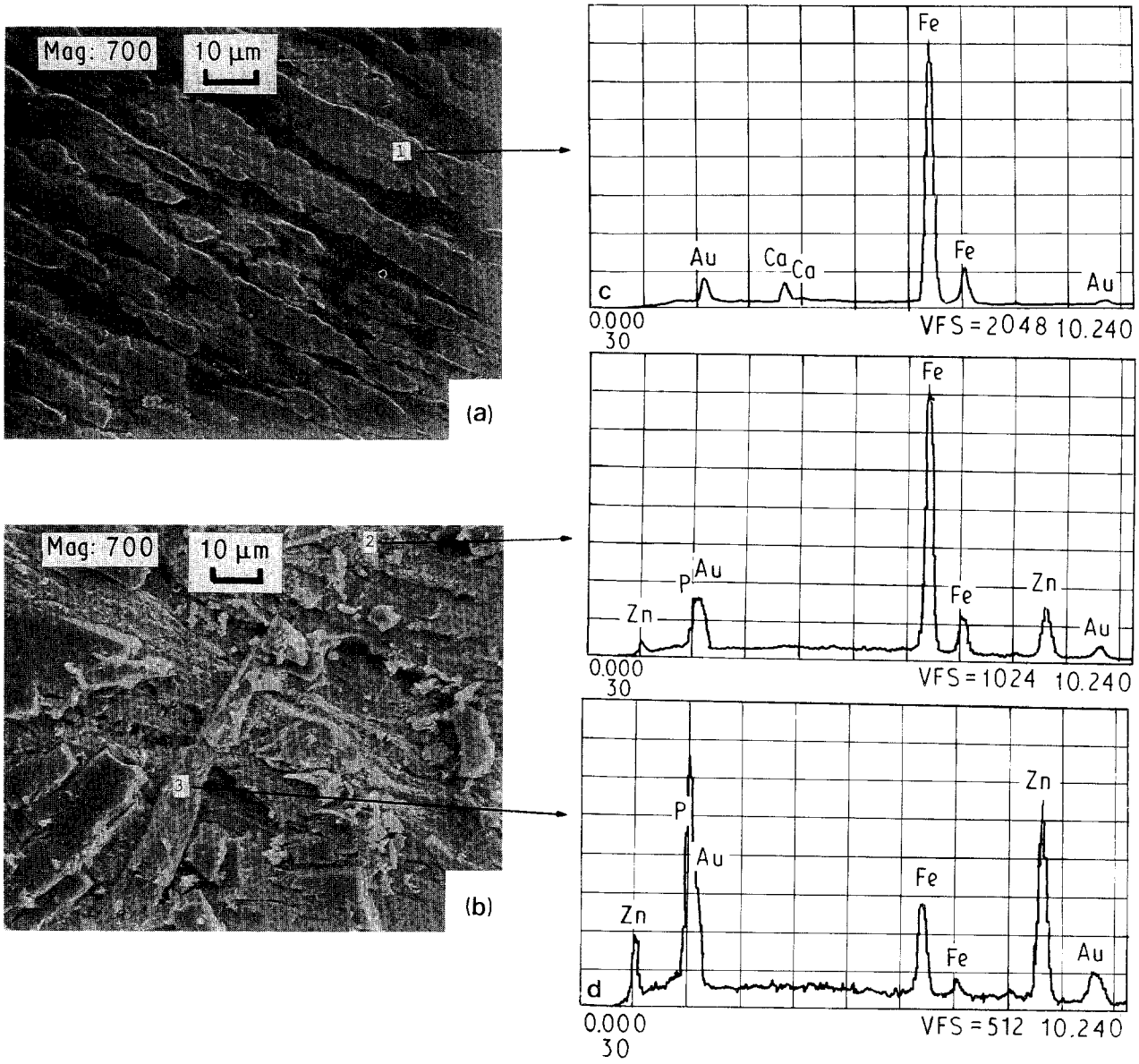

Figure 2 (a, b) High-resolution SEM images coupled with EDX of (c) as-received fibre, and (d) ZnPh-deposited fibre.

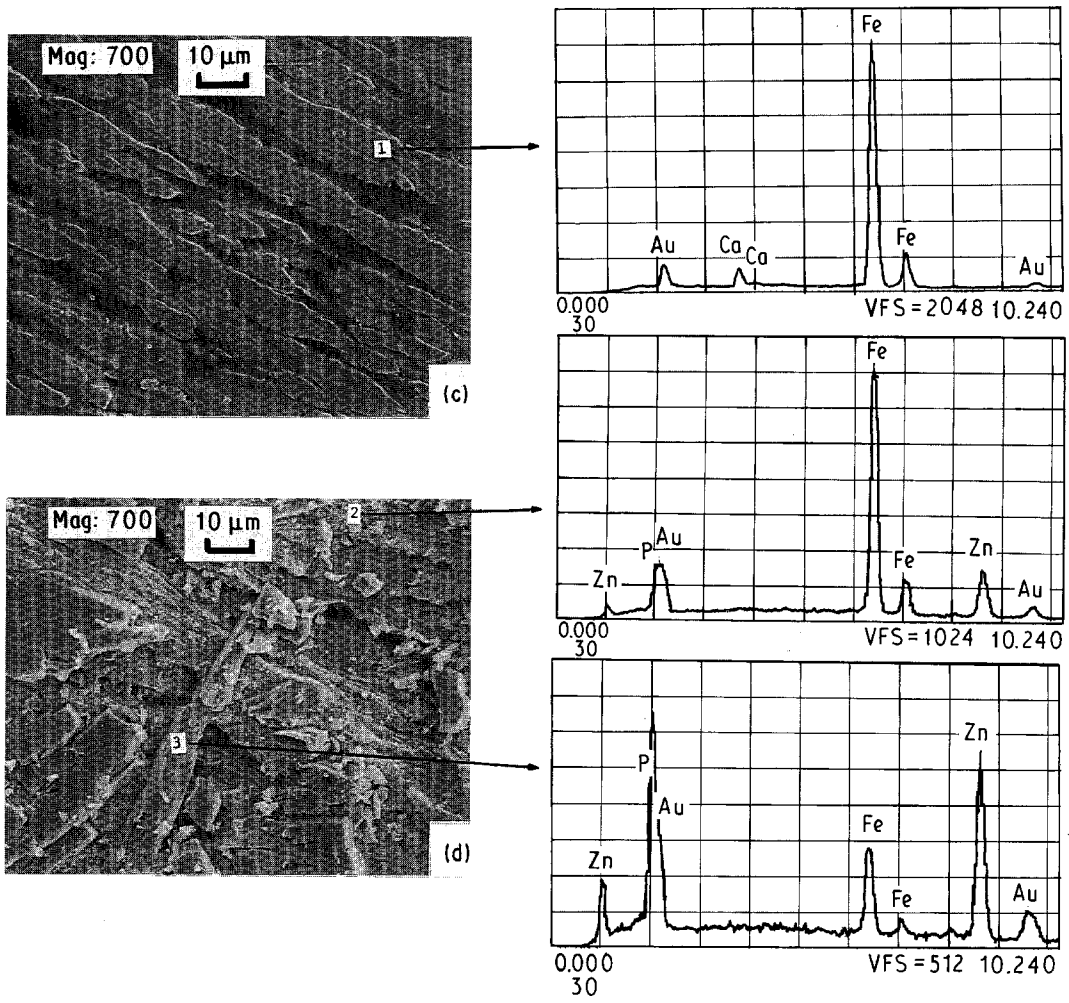

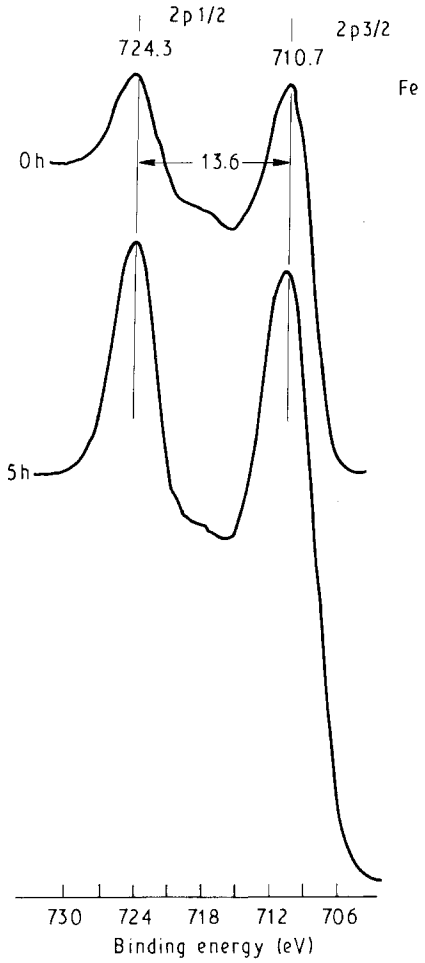

Figure 3 High-resolution Fe_{2p} separation XPS spectra for unexposed and 5 h exposed as-received fibres in NaCl solution.

same BE positions can be seen from the 5 h samples, suggesting that the fibre surface was significantly corroded during 5 h of exposure.

On the basis of this information, we made a quantitative evaluation of elements for the ZnPh-treated fibre surfaces before and after exposure: Table II gives these data. For the unexposed ZnPh surface, the quantitative distributions of C, O, P, Zn, and Fe were 48.9%, 41.6%, 3.1%, 2.2% and 4.2%, respectively. After exposure, the concentrations of Fe and C atoms tended to decrease with increased exposure, while the proportions of O, P, and Zn increased during exposures up to 24 h. The immersion of ZnPh-coated fibres in the NaCl solution results in an extensive elimination of the Fe and C atoms at the outermost surface sites of the conversion coatings. However, we did not explore this further. Although it cannot be seen in any of our figures and tables, no increase in signal intensity was found at 710.7 and 724.3 eV in the Fe_{2p} region of the 24 h exposed ZnPh samples, that might reflect the

TABLE II Changes in the chemical composition of the surface of ZnPh-treated steel fibres after exposure to 3% NaCl at 25 °C

Exposure time (h)	At %				
	C	O	P	Zn	Fe
0	48.9	41.6	3.1	2.2	4.2
1	47.9	41.2	5.6	2.7	2.6
2	45.5	41.2	8.0	3.7	1.6
5	44.1	42.8	8.4	3.7	1.0
24	43.4	43.6	8.0	3.5	1.5

formation of ferric rust. Thus, the ZnPh coatings appear to provide good corrosion protection to the steel fibres.

3.2. Adhesion and interface between ZnPh-treated fibre and cement paste

To investigate the adherence of ZnPh to the cement pastes, the bond strength at the fibre–cement interfaces was determined from the pull-out load of a single fibre embedded in the cement matrix. The results, shown in Table III, are compiled as a function of the cement hydration ages at 25 °C. The pull-out behaviour of both the ZnPh-treated and untreated fibres depended on the hydration ages of pastes; that is, the value of the tensile load of fibres in an aged cement was higher than that of a 3 day specimen. We verified that the surface of the ZnPh-deposited fibre adhered well, improving bond strength by 40% over that of untreated fibres. This result suggests that the ZnPh precipitated on the steel fibre promotes strong interfacial bonding at the fibre–cement boundaries.

Because one of our research objectives was to understand better the adhesion mechanism and the structure contributing to the strong bond, we focused on microstructure development, chemical composition and state in the fibre–cement interfacial regions of the 28 day aged specimens. These factors were investigated with the combined analytical techniques of SEM with EDX, and XPS.

For the SEM–EDX studies, the removed fibre was first washed in deionized water to eliminate any unbound cement paste from the surface, and then dried at 110 °C for 24 h. Fig. 4 shows the SEM–EDX observation of the as-received fibre after pull-out. Most of the fibre's surface was devoid of massive cement hydration products, and only locally adhering paste particles could be seen on close inspection (Fig. 4b). The EDX spectrum of an agglomerate particle, denoted as area 4, is representative of the enrichment of Ca as the dominant chemical constituent, suggesting that the enriched Ca element may come from either the formation of $CaCO_3$, or $Ca(OH)_2$, or both. The SEM–EDX inspections of a groove in the paste, created by the fibre being pulled away from the cement matrices, are shown in Fig. 5. The scanning electron micrograph of the groove wall, marked as site 7, shows the dense lining morphology of the packed cement pastes; the features of the EDX spectrum accompanying the micrograph were similar to those from the pull-out fibre surface described above (Fig. 4). The latter result suggests that the chemical composition of the groove surface consists of the $CaCO_3$ and $Ca(OH)_2$. Site 8, located at a distance of $\sim 100\ \mu m$ from the edge of groove, was ascertained from EDX analysis to be the CaO–SiO_2–H_2O system of the cement matrix, because it showed a lower peak-count ratio of Ca/Si compared with that of site 7. However, an important question that remains is which one of two Ca-based compounds, $CaCO_3$ and $Ca(OH)_2$, preferentially precipitates on the steel fibres during the induction period of cement hydration? Explorative work to answer this question was performed using XPS high-resolution techniques which can identify specific chemical compounds and states formed in surface layers up to 0.5 nm thick. With this technique, it is possible to find a near-monolayer of Ca compounds precipitated on fibre surfaces at atomic levels. The samples for XPS examination were prepared by

TABLE III Pull-out load of untreated and ZnPh-treated fibres embedded in aged cement pastes

	Age of cement (days)	Pull-out load (N)
Untreated fibre	3	236
	14	250
	28	275
ZnPh-treated fibre	3	331
	14	356
	28	380

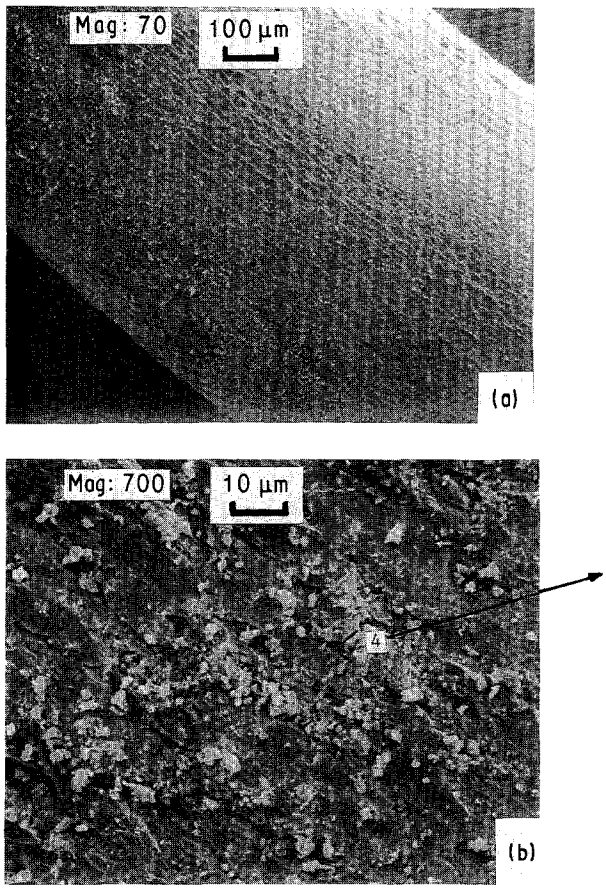

Figure 4 SEM–EDX analysis of as-received fibre surface removed from 28 day aged cement pastes.

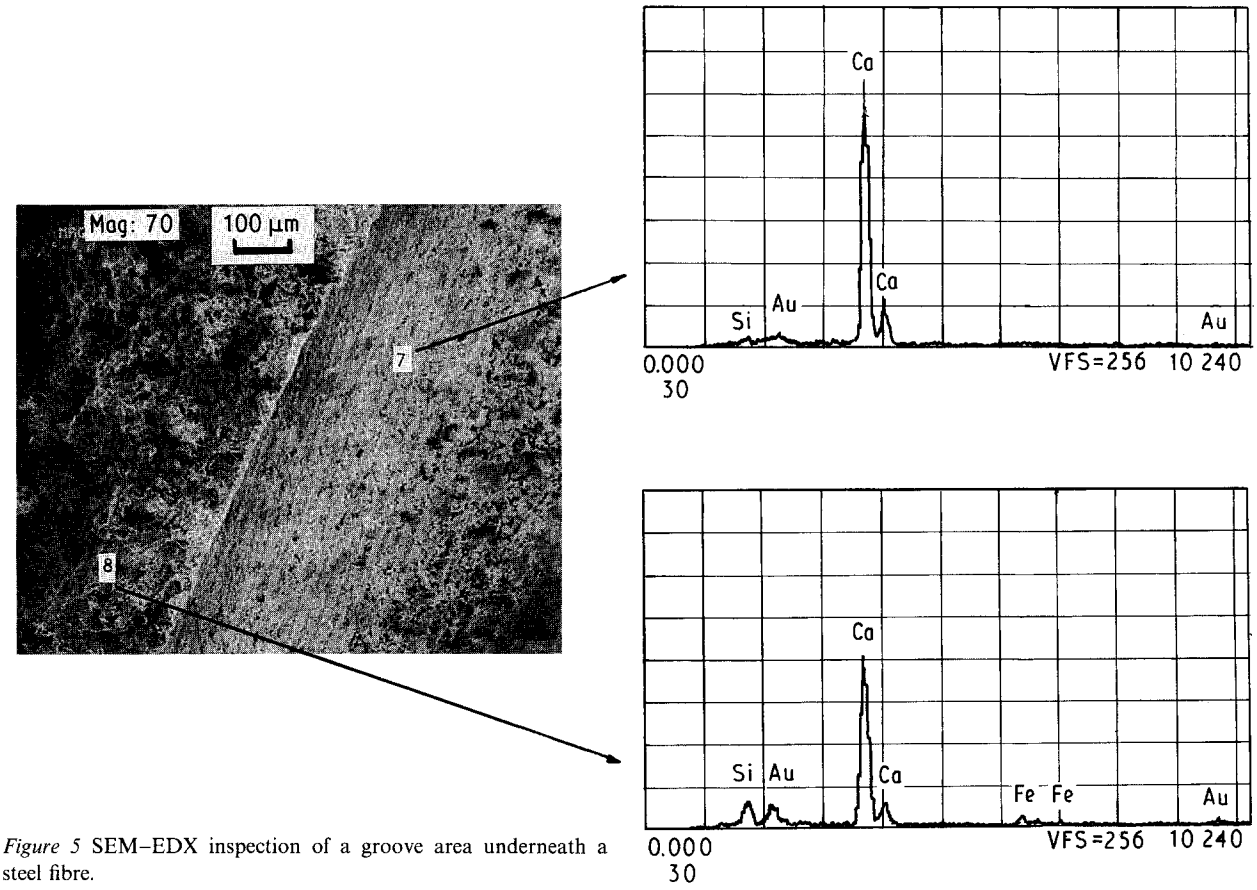

Figure 5 SEM–EDX inspection of a groove area underneath a steel fibre.

immersing the fibres in centrifugally extracted Type 1 cement aqueous solution. This cement solution was made by adding 50 g Type 1 cement to 25 ml deionized water. After mixing for 30 min at 25 °C, the cement suspension phase was extracted by centrifugal separation, and then the extracted aqueous phase was filtered. The Ca ion content of the filtered cement solutions having a pH value of 13 was determined by atomic absorption spectrophotometry; the resultant concentration of Ca was 2.4 $\mu mol\,l^{-1}$.

Fig. 6 shows the changes in the spectrum of $Ca_{2p3/2}$ core level as a function of the immersion times up to 2 h. The spectrum of the fibre surface exposed for 30 min exhibits three resolvable peaks, consisting of two major peaks at 347.4 and 346.9 eV, and an appreciable shoulder signal at 347.7 eV. One of the major lines at 347.4 eV can be ascribed to Ca in the contaminated compounds, and the other clearly reveals the Ca in $CaCO_3$ formations [15]. The shoulder at 347.7 eV is due to Ca in $Ca(OH)_2$ formations. This finding strongly demonstrated that the amount of $Ca(OH)_2$ precipitated on the fibre's surface is very small compared with the amount of $CaCO_3$. The magnitude in intensity of both the $CaCO_3$ and $Ca(OH)_2$ calcium peaks significantly increases between exposure times of 30 min and 1 h, whereas the Ca contaminant peak vanishes after immersion for 1 h. This result implies that the Ca contaminants were completely covered with the mixed Ca-based compounds consisting of $CaCO_3$ as a major phase and $Ca(OH)_2$ as a minor one. As a result, we believe that when Ca^{2+} ions released from the hydrated cement grains reach the fibre surface, they preferentially react with CO_3^{2-}, reactants in the cement solutions, and then form $CaCO_3$. The conversion rates to $CaCO_3$ of Ca^{2+} in the vicinity of the fibre surface appear to be much higher than the rate of Ca to $Ca(OH)_2$ transformations. Further extending the exposure time to 2 h results in an increase in the extent of precipitation of the $Ca(OH)_2$ signal intensity at 347.7 eV. By contrast, the line intensity at 346.9 eV drastically diminishes, thereby suggesting that the $Ca(OH)_2$ layer covers the underlying $CaCO_3$ phases during 2 h exposures.

As is well documented [16], steel surfaces are commonly overlaid by a passive film which provides inherent protection against corrosion. The passive film

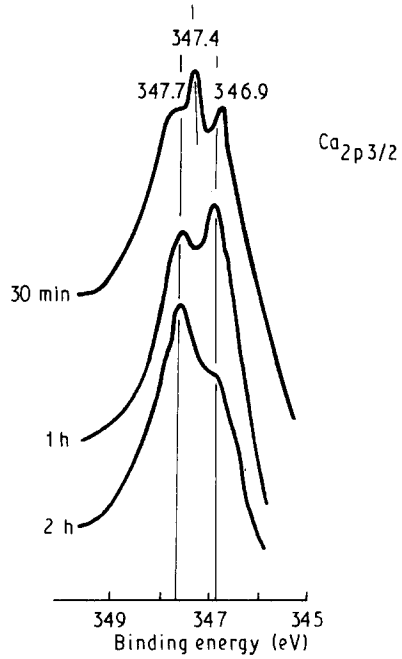

Figure 6 $Ca_{2p3/2}$ region for steel fibres immersed in cement solution.

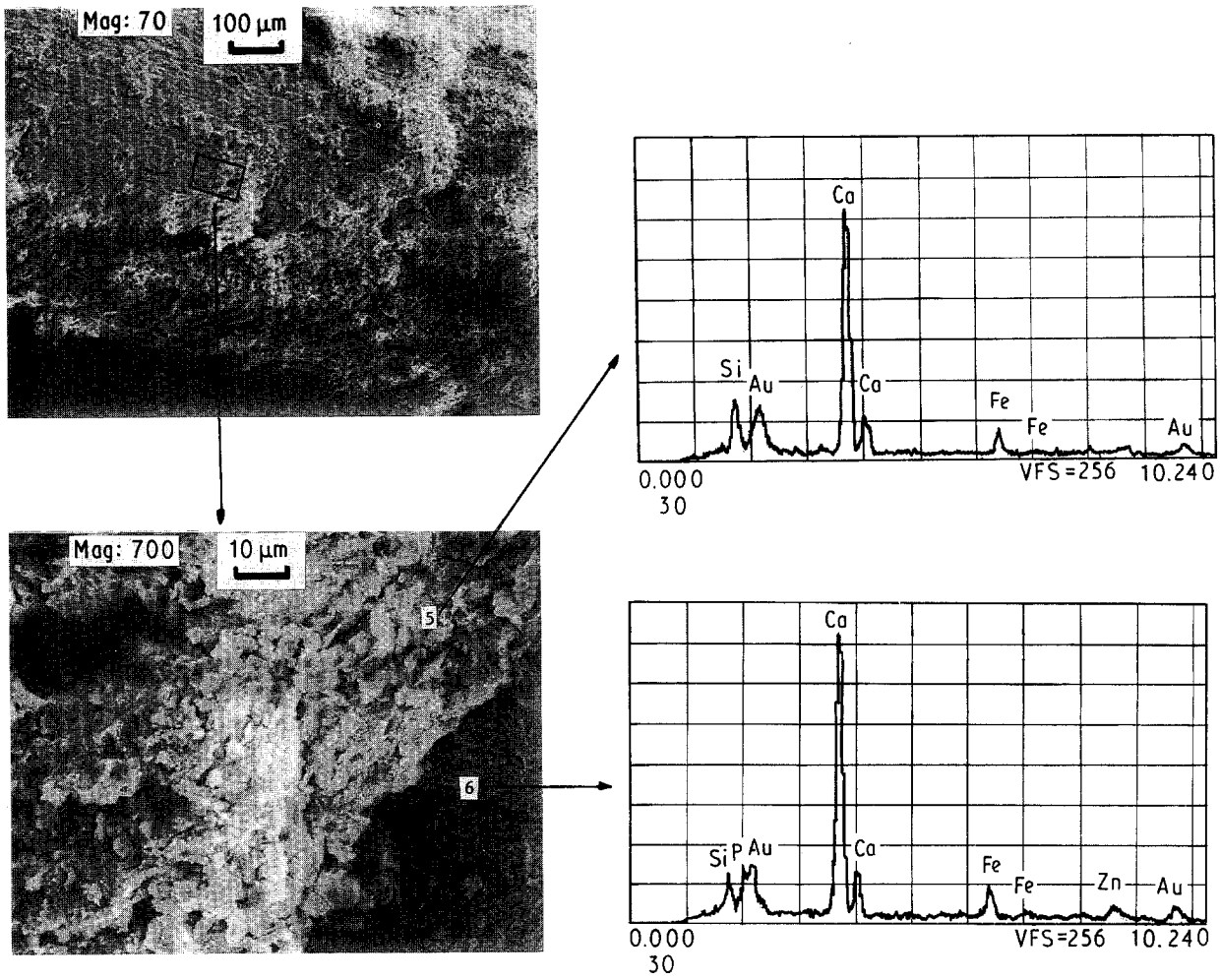

Figure 7 SEM–EDX images of the surface of a pulled-out ZnPh-treated fibre.

is very stable at high pH. However, a drop in pH results in the removal of the passive film, and so the steel corrodes. Hence, although the pH of cement paste is high, preferential depositions of $CaCO_3$ on surfaces of the steel fibres may reduce the pH value in the vicinity of the fibres [17]. The decrease in pH consequently results in the corrosion of the fibres.

Based upon our knowledge of the untreated fibre–cement interfacial regions, considerable attention was paid to the critical interfacial zone between the ZnPh-treated steel fibre and the 28 day aged cement paste. Fig. 7 shows the SEM image with the EDX elemental analysis for the ZnPh-treated fibre surface removed from the cement matrix. The microstructure clearly indicated that the tensile failure of the fibre–cement bond occurs both at the interface and in the bulk of the cement paste, leaving the hydration products adhering to ZnPh surface, and thereby suggesting that there was a good interfacial bond. From the EDX spectrum taken at site 5, the massive cement hydrates, composed of agglomerated plate-like crystals, seem to be associated with the $CaO–SiO_2–H_2O$ system of the hydraulic cement matrices. In contrast, there was no sign of the presence of remaining massive cement pastes at site 6. EDX examination of this area revealed that Ca was the dominant element, and Si, P, Fe, and Zn were minor ones, implying that the ZnPh coating was covered with Ca-based compound layers of a certain thickness. Because EDX is used to detect surface solid layers up to ~ 2 μm thick, we estimated that the thickness of the covered Ca compound layers was no more than 2 μm. The surface of the groove after the treated fibre was pulled away was also subjected to SEM–EDX inspection (Fig. 8). The topographical image of the groove denoted as site 9 disclosed that the microtexture of the compacted paste is similar to that from site 7 in Fig. 5. Although the intensity of the peak signal on the EDX spectrum of site 9 is weak, the spectrum particularly indicated the presence of an appreciable amount of P element. The detection of such an element on the sides of the grooves suggests that there is a migration of elemental P from the ZnPh coatings into the cement matrix. This migration seems to be associated with the dissolution of crystalline coatings caused by the attack of a high pH interstitial fluid in the vicinity of the cement pastes. Assuming that alkali dissolution of ZnPh coatings occurs at a critical contact zone, it is worthwhile to explore the chemical behaviour of the ionic species dissociated from the coating surfaces. Our emphasis was on investigating the reactivity of the dissociated ionic species with the cement pastes, and then to identify the interaction products formed at the contact zones of the ZnPh–hydraulic cement. Inevitably, attention was paid to evaluating the protection against corrosion afforded by the reaction products acting as barriers to reactants in the environment.

XPS was used to obtain all this information. The samples for the XPS studies were prepared by soaking the ZnPh-treated fibres in filtered Type 1 cement solutions at pH 13.0. The soaked fibres then were rinsed with a deionized water, and dried at 110 °C for 20 h.

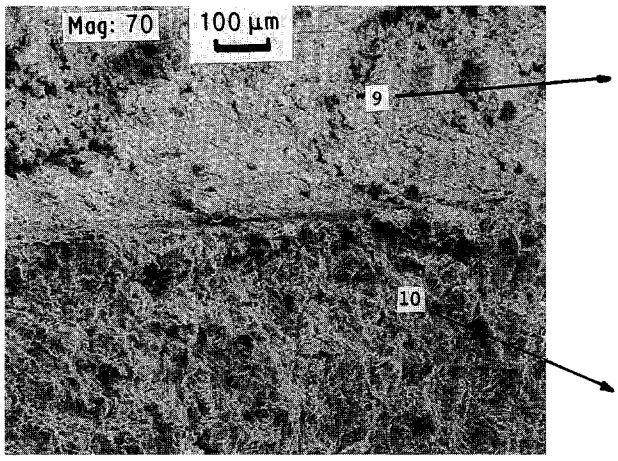

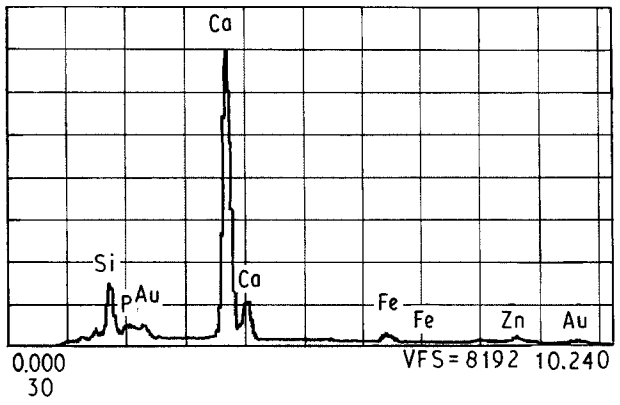

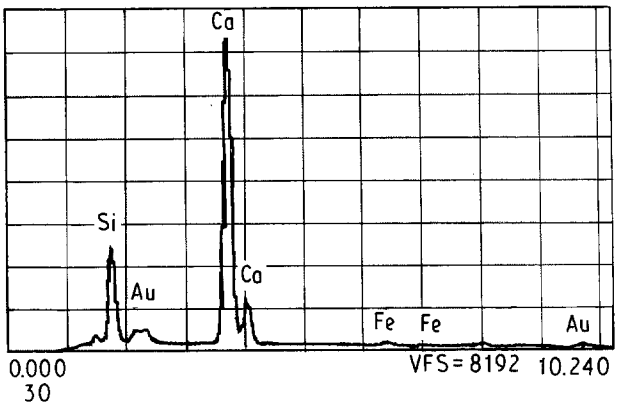

Figure 8 SEM–EDX of a groove area underneath a ZnPh-deposited steel fibre.

Table IV shows the changes in elemental composition of ZnPh-deposited fibre surfaces as a function of exposure times. As discussed earlier, we already knew that the dissociation rate of PO_4^{3-} ions is much higher than that of Zn^{2+} when the ZnPh was exposed to NaOH solutions. This difference was reflected directly in the XPS quantitative data. Thus, the proportion of P atoms at the surface increased markedly during a soaking period of 2 h; beyond this time, the proportion seems to decrease. A similar trend, with the exception of a continuous increase in atomic concentration after exposure for 2 h, was observed from the Ca element. In contrast, the concentration of Zn and Fe atoms significantly dropped in the first 30 min exposure. These data demonstrated that the principal reaction products formed at the critical interfacial zones between the cement solution and the dissolved ZnPh were likely to be associated with the calcium phosphate compounds continually precipitated on the alkali-damaged ZnPh surfaces. However, further exposure up to 5 h seemed to slow down the rate of precipitation, implying that severe alkali-dissolution of ZnPh no longer occurs.

Next, the XPS study focused on the identification of the insoluble calcium phosphate compound phases precipitated on the fibre surface over the 5 h exposures. Other papers [11, 12] have suggested that hydroxyapatite, $[Ca_5(PO_4)_3(OH)]$, and brushite, $(CaHPO_4 \cdot 2H_2O)$ may be formed. However, there are no reports of high-resolution XPS studies of such

TABLE IV Surface composition of ZnPh-coated steel fibre as a function of exposure time to cement solution at pH 13

Exposure time (h)	At %					
	P	C	Ca	O	Fe	Zn
0	3.1	48.9	0.0	41.6	4.2	2.2
0.5	3.9	51.7	2.8	40.7	0.4	0.5
1.0	4.2	40.9	3.8	49.7	0.8	0.6
2.0	5.1	41.3	4.8	47.1	0.6	0.7
5.0	3.3	43.6	5.7	46.0	0.7	0.7

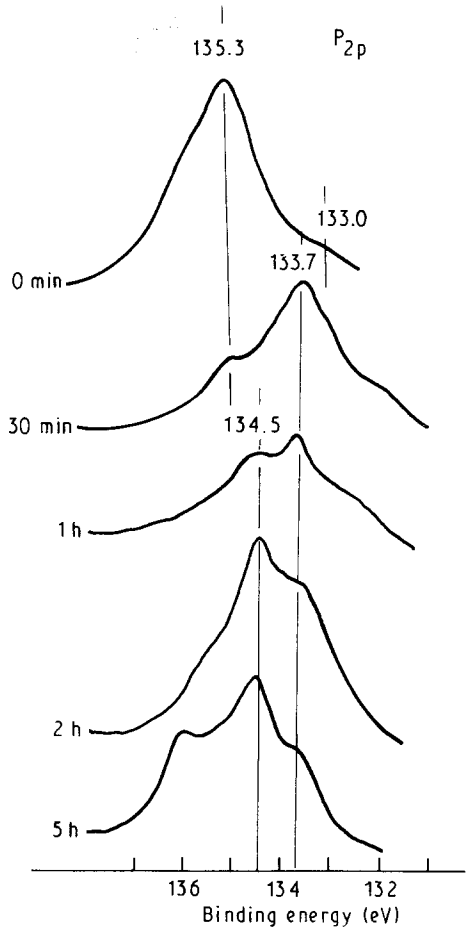

Figure 9 Changes in the P_{2p} peaks of ZnPh-covered steel fibre surfaces after exposure to a cement solution (pH = 13).

compounds. Thus, we used these compounds of chemical reagent grades (supplied by Alfa), as reference compounds in our attempt to identify the BE of the precise peak positions in the P_{2p} and $Ca_{2p3/2}$ regions. The peak positions from the P_{2p} and $Ca_{2p3/2}$ spectra of the reference compounds were: 133.6 eV in P_{2p} and 347.7 eV in $Ca_{2p3/2}$ regions for $Ca_5(PO_4)_3(OH)$, and 134.4 eV in P_{2p} and 348.7 eV in $Ca_{2p3/2}$ core levels for $CaHPO_4 \cdot 2H_2O$.

XPS spectra of the P_{2p} region from these sample surfaces are illustrated in Fig. 9. The signal from the ZnPh-treated fibre before soaking could be resolved into two Gaussian components at 135.3 and 133.0 eV peaks. The former peak, corresponding to the principal component, is assignable to the P in the conversion coatings; the assignment of the shoulder peak at 133.0 eV has not been resolved. An additional phosphate compound is clearly introduced into the ZnPh surfaces after immersion for 30 min; the spectrum then shows a prominent peak at 133.7 eV, reflecting the formation of this new phosphate compound. By comparison with the peak position differences of the reference compounds, we confirmed that the major contributor to this new peak was P in hydroxyapatite. Extended immersion times to 1 h led to the formation of another phosphate compound, recognized by the peak signal emerging at 134.5 eV. According to the reference peaks, this new signal may be due to the P in the brushite formations. Further, the doublet signal feature of a 1 h aged spectrum revealed the presence of two major phosphate compounds, $Ca_5(PO_4)_3(OH)$ and $CaHPO_4 \cdot 2H_2O$. An attenuation of signal intensity at 135.3 eV, originating from the P in the conversion coatings, suggested that the hybrid formations of these Ca phosphate compounds as the reaction products of the interfacial reactions between the Ca ions from the hydraulic cement and the PO_4^{3-} ions from the conversion coatings, are precipitated on the outer surface of coatings after a 1 h exposure. In other words, the damaged areas of coatings caused by alkali dissolution might be repaired by the precipitations of these reaction products. The spectra from the 2 h exposed sample surfaces suggests that further prolonged exposure leads to a conspicuous growth of signal intensity at 134.5 eV, and to a decay of the hydroxyapatite peak at 133.7 eV. We think that this represents the interaction of Ca ions with the abundant PO_4^{3-} ions that dissociate from the coatings in the first 30 min exposure and preferentially cause the formation of hydroxyapatite, rather than of brushite at the dissolved ZnPh surfaces. Once the precipitation of hydroxyapatite on ZnPh commences, it prohibits further dissociation of PO_4^{3-} ions. Thus, a lower concentration of PO_4^{3-} in the vicinity of the hydroxyapatite-precipitated ZnPh surfaces leads to the formation of brushite as a principal phase in extended periods of exposure.

To verify this hypothesis, we inspected the $Ca_{2p3/2}$ core level region for these samples (Fig. 10). The spectrum from the sample surface after 30 min immersion consists mainly of an intense signal at 347.7 eV and a weak line at 348.7 eV. The former peak as a major phase corresponds to Ca in the hydroxyapatite formations, and the latter reveals the presence of brushite as a minor phase. As expected, prolongation of exposure resulted in a pronounced increase in a signal intensity at 348.7 eV, while the peak at 347.7 eV decays.

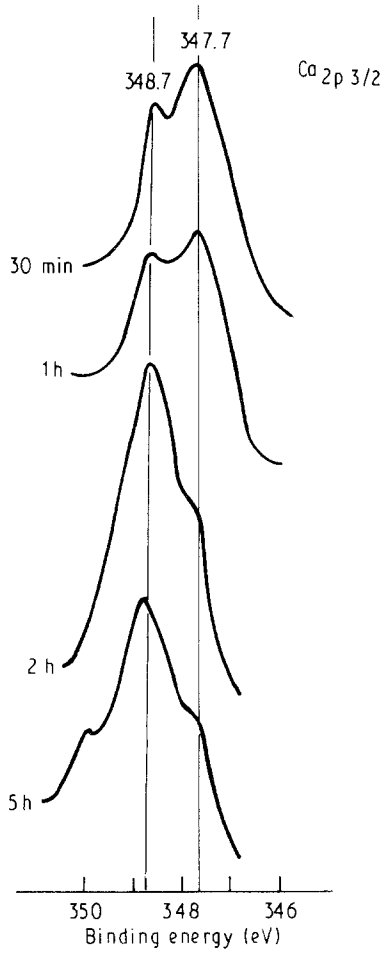

Figure 10 Changes in the $Ca_{2p3/2}$ peaks of ZnPh-treated fibre surfaces after exposure to a cement solution.

The XPS data clearly showed that the precipitation rates of hydroxyapatite to brushite depend on the concentrations of dissociated PO_4^{3-} ions at the cement solution–ZnPh interfacial contact. For short exposures, the extent of alkali dissolution of ZnPh is predicted to be very high, so that the diffusion of a large amount of PO_4^{3-} ion into the cement fluids promotes the precipitation of hydroxyapatite with three PO_4 components in the molecular structure. Assuming that the hydroxyapatite layer precipitated on the dissolved ZnPh acts as a barrier to alkali reactants, then further dissolution of the coatings can be reduced. Hence, the reduced liberation of PO_4^{3-} ions, which occurs during prolonged exposure, substantially induces the formation of brushite, with one PO_4, on top of the hydroxyapatite layers. We believe that such a dissolution interaction mechanism occurring at the fibre–cement contact zones plays an important role in forming the intermediate cross-linking structure which may serve to rejoin the fibre with the cement paste.

An important question still remains that concerns the ability of such Ca-based compounds to protect the steel fibre from corrosion. To estimate this protection, both ZnPh-treated and untreated fibres were immersed in a filtrated cement solution for 5 h, and then exposed to an aerated 3.0% NaCl solution for up to

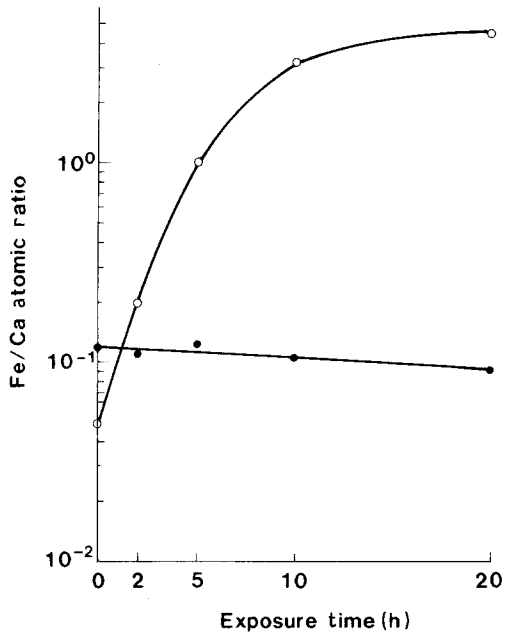

Figure 11 Changes in Fe/Ca ratio with NaCl exposure times for the (●) ZnPh-treated and (○) untreated steel fibre surfaces after exposure to cement solution for 5 h.

24 h. After 5 h in cement, the "as-received" steel fibre surface was coated with mixed formations of $Ca(OH)_2$ and $CaCO_3$, and the surface of the ZnPh coating had some coverage with hybrid calcium phosphate compound layers consisting of $Ca_5(PO_4)_3(OH)$ and $CaHPO_4 \cdot 2H_2O$. XPS elemental quantitative analyses were carried out on the corrosion-induced chemical changes. Two elements were selected for analysis, Fe which is assignable to the formation of ferric rust compounds, and Ca that reflects the Ca-based anticorrosive layers. Because an increase in Fe concentration in samples exposed to NaCl solution reflects an increased amount of rust products, and enhancement of corrosion rates, the variations in Fe to Ca atomic ratio were investigated as a function of NaCl exposure times (Fig. 11). The data indicate that the multi-protective layers, consisting of the $Ca_5(PO_4)_3(OH)$ and $CaHPO_4 \cdot 2H_2O$ that are superimposed upon the dissolved ZnPh layer, serve as a barrier to NaCl reactant. Thus, the results show no significant changes in Fe/Ca ratio after 24 h, but, in contrast, the Fe/Ca ratio for the $Ca(OH)_2$–$CaCO_3$ composite layers precipitated on the as-received fibre markedly rise as exposure time is prolonged. This finding verified that the protective ability of such layers is very poor. In fact, the red–brown rust products can be seen on the fibre surfaces after exposures longer than 5 h.

Therefore, the intermediate calcium phosphate compound layers formed by the interaction between Ca^{2+} ions and PO_4^{3-} ions dissociated from the ZnPh not only contribute to an increase in the strength of the fibre–cement interfacial bonds, but also play an important role in repairing the areas of the damage in the anticorrosive ZnPh layers brought about by alkali dissolutions.

4. Conclusion

A 150 °C-heated ZnPh layer deposited on the surface of steel fibres provided considerable protection against the corrosive attack of NaCl. When the ZnPh-deposited steel fibres were incorporated into cement pastes, the greater susceptibility of ZnPh to the alkali-induced dissolution resulted in the dissociation of abundant PO_4^{3-} ions at the critical interfacial zone between the ZnPh and the paste. These PO_4^{3-} ions chemically react with the nucleophilic Ca^{2+} ions from the paste, and, subsequently, transform into hydroxyapatite as the initial reaction product close to the cement alkali-dissolved ZnPh surface. The hydroxyapatite layer probably prohibits further dissolutions of ZnPh, resulting in the secondary precipitation of brushite caused by a reducton in PO_4^{3-} dissolution. Such intermediate interaction products formed at the cement paste–ZnPh interfaces not only enhance the cement–fibre adhesive forces, but also play an important role in repairing the alkali-damaged areas of ZnPh. The latter effect reflected directly on the corrosion protection of fibres.

In contrast, the surfaces of as-received steel fibres which come into contact with cement pastes seem to be covered by the hybrid compounds of $CaCO_3$ and $Ca(OH)_2$ phases. However, these compounds have no significant effect in protecting the fibres against corrosion.

Acknowledgement

This work was performed under the auspices of the US Department of Energy, Washington, DC, under Contract No. DE-AC02-76CH00016.

References

1. T. SUGAMA, L. E. KUKACKA, N. CARCIELLO and J. B. WARREN, *J. Mater. Sci.* **23** (1988) 101.
2. T. SUGAMA, in "Adhesives, Sealants, and Coatings for Space and Harsh Environments", edited by L. H. Lee Vol. 37 (Plenum Press, New York, 1988) pp. 405–30.
3. T. SUGAMA, L. E. KUKACKA, N. CARCIELLO and J. B. WARREN, *J. Coating Technol.* **61** (1989) 43.
4. C. TASHIRO and K. UEOKA, *Cem. Concr. Res.* **11** (1981) 619.
5. C. TASHIRO and S. TATIBANA, *ibid.* **13** (1983) 337.
6. A. MACIAS and C. ANDRADE, *Brit. Corros. J.* **22** (1987) 113.
7. *Idem., ibid.* **22** (1987) 119.
8. A. J. SOMMER and H. LEIDHEISER Jr, *Corrosion* **43** (1987) 661.
9. N. L. THOMAS, *J. Mater. Sci.* **22** (1987) 3328.
10. R. S. BARNEYBACK Jr and S. DIAMOND, *Cem. Concr. Res.* **11** (1981) 279.
11. G. K. HUNTER, B. L. ALLEN, M. D. GRYNPAS and P. T. CHENG, *Biochem. J.* **228** (1985) 463.
12. K. KOMIYA, T. YOKO, K. TANAKA and Y. FUJIYAMA, *J. Mater. Sci.* **24** (1989) 827.
13. J. T. KEISER, C. W. BROWN and R. H. HEIDERSBACH, *Corrosion* **38** (1982) 357.
14. N. S. McINTYRE and D. G. ZETARUK, *Anal. Chem.* **49** (1977) 1521.
15. C. D. WAGNER, W. M. RIGGS, L. E. DAVIS and J. F. MOULDER, "Handbook of X-Ray Photoelectron Spectroscopy" (Perkin-Elmer Corporation, 1979) p. 64.
16. C. M. HANSSON, *Cem. Concr. Res.* **14** (1984) 574.
17. C. L. PAGE and K. W. J. TREADAWAY, *Nature* **297** (1982) 109.

Received 15 June
and accepted 26 June 1990